Numerical solution of the t–J model with random exchange couplings in d=∞ dimensions

Junya Otsuki, Dieter Vollhardt

Angaben zur Veröffentlichung / Publication details:

Otsuki, Junya, and Dieter Vollhardt. 2013. "Numerical solution of the t–J model with random exchange couplings in d=∞ dimensions." *Physical Review Letters* 110 (19): 196407. https://doi.org/10.1103/physrevlett.110.196407.

Numerical Solution of the t-J Model with Random Exchange Couplings in $d = \infty$ Dimensions

Junya Otsuki[1,2] and Dieter Vollhardt[1]

[1]*Theoretical Physics III, Center for Electronic Correlations and Magnetism, Institute of Physics, University of Augsburg, D-86135 Augsburg, Germany*

[2]*Department of Physics, Tohoku University, Sendai 980-8578, Japan*

(Received 19 December 2012; published 10 May 2013)

To explore the nature of the metallic state near the transition to a Mott insulator, we investigate the t-J model with random exchange interaction in $d = \infty$ dimensions. A numerically exact solution is obtained by an extension of the continuous-time quantum Monte Carlo method to the case of a vector bosonic field coupled to a local spin. We show that the paramagnetic solution near the Mott insulator describes an incoherent metal with a residual moment, and that single-particle excitations produce an additional band, which is separated from the Mott-Hubbard band.

DOI: 10.1103/PhysRevLett.110.196407 PACS numbers: 71.30.+h, 71.10.Hf, 75.10.Nr

The extraordinary properties of high-T_c cuprates are closely related to those of doped Mott insulators [1,2]. In both systems, strong electronic correlations play a key role. To understand their influence, fundamental electronic correlation models such as the Hubbard and the t-J model have been studied intensively [2]. In spite of their apparent simplicity, these quantum mechanical many-particle models can only be solved approximately in dimensions $d = 2, 3$. Thus, the full range of physical phenomena described by the Hubbard or the t-J model is not yet understood, implying that their investigation still leads to unexpected, and often peculiar results. For example, it has been pointed that the Fermi-surface volume of the two-dimensional t-J model is inconsistent with the Luttinger-Ward theorem [3–6]. Indeed, by applying the Schwinger method to the t-J model, Shastry [7] recently found a class of solutions which show precisely such a behavior. In this situation, it is desirable to obtain reliable conclusions about those correlation models at least in certain solvable nontrivial limits. In the case of doped Mott insulators, "nontrivial" means that characteristic features such as a strong, but screened Coulomb repulsion and the presence of local spin fluctuations in real space are retained. Namely, the screened Coulomb interaction is responsible for the Mott metal-insulator transition (MIT), and local spin fluctuations affect the quasiparticles by making the self-energy frequency dependent.

The Mott MIT can be described by the dynamical mean-field theory (DMFT) [8,9]. The DMFT provides an exact, nontrivial solution of electronic lattice models with a local interaction such as the Hubbard model, in $d = \infty$. It can be derived by mapping the original quantum lattice problem onto an effective quantum impurity coupled self-consistently to a dynamical fermionic mean-field ("bath") [9]. However, due to the local nature of the DMFT *intersite* interactions are reduced to a static mean field. This implies that in the strong-coupling limit of the Hubbard model, which corresponds to the Heisenberg model in the case of half filling and to the t-J model in the doped case, nonlocal spin fluctuations are missing. At the same time, it is known from the investigation of spin models in the context of spin-glass problems, that when the spin coupling J_{ij} is taken to be *random*, nonlocal spin fluctuations survive even in $d = \infty$, while the static mean field averages out [10–16]. In this case, the self-consistency equations correspond to those of an effective impurity problem coupled to a bosonic bath. In particular, the random-coupling Heisenberg model has a very remarkable property: as shown by Sachdev and Ye [13] for SU(M) spins with $M = \infty$, its dynamical magnetic susceptibility displays marginal Fermi liquid behavior, which was proposed in the phenomenological theory for the cuprate superconductors [17]. This suggests a relation of the random-coupling Heisenberg model to the paramagnetic state of the cuprates. Indeed, spin-glass behavior was observed in $La_{2-x}Sr_xCuO_4$ in the low-doping regime $x = 0.04$ [18,19].

The effect of doping on the random-coupling Heisenberg model was studied in detail by Parcollet and Georges [20] in terms of the t-J model with random couplings J_{ij} in the limit $M = \infty$. This model also has a nontrivial $d = \infty$ limit and describes a doped Mott insulator without antiferromagnetic spin fluctuations. In particular, these authors calculated the coherence scale of quasiparticles and discussed the properties of an incoherent metallic state near half filling.

In this Letter, we present a numerically exact solution of the random coupling t-J model for the realistic number of spin components, $M = 2$. This is made possible by an extension of the continuous-time quantum Monte Carlo (CT-QMC) method to a local spin coupled to a bosonic field. We compute the quasiparticle energy scale as a function of doping and determine the spectrum of the incoherent metal near the Mott insulating state.

The random coupling t-J model in $d = \infty$.—To obtain a nontrivial $d = \infty$ limit (in the following, we use the coordination number $Z = \infty$ instead) where nonlocal spin

fluctuations are retained, the coupling constants J_{ij} should be scaled as $J_{ij} = J^*_{ij}/\sqrt{Z}$, with $J^*_{ij} = \text{const}$ [20–22], in complete analogy to the scaling of the hopping amplitude [8,9]. However, since the static molecular field is proportional to ZJ, the above scaling leads to a divergence of the transition temperature for magnetic long-range order at half filling; i.e., the paramagnetic state is unstable against an infinitesimally small external field for all finite temperatures. This problem does not occur when the coupling constants J_{ij} are random variables, since then $\sum_j J_{ij} = 0$ but $\sum_j J^2_{ij} \neq 0$, implying that the static molecular field due to the surrounding sites averages to zero [11]. Doping of the random coupling Heisenberg model then leads to the random coupling t-J model [20]

$$H = -\frac{t}{\sqrt{Z}} \sum_{\langle ij\rangle\sigma} \tilde{c}^\dagger_{i\sigma}\tilde{c}_{j\sigma} - \frac{1}{2}\sum_{\langle ij\rangle} \frac{J_{ij}}{\sqrt{Z}} \boldsymbol{S}_i \cdot \boldsymbol{S}_j, \tag{1}$$

where $\tilde{c}_{i\sigma} = c_{i\sigma}(1 - n_{i-\sigma})$, $\boldsymbol{S}_i = (1/2)\sum_{\sigma\sigma'} c^\dagger_{i\sigma}\boldsymbol{\sigma}_{\sigma\sigma'}c_{i\sigma'}$. Here, the summation is taken over nearest-neighbor sites, and we consider the Bethe lattice with infinite connectivity ($Z = \infty$) [23]. The exchange couplings J_{ij} are randomly distributed according to the probability distribution

$$P(J_{ij}) \propto \exp(-J^2_{ij}/2J^2). \tag{2}$$

Neglecting spin-glass order, the model defined by Eq. (1) with $Z = \infty$ reduces to an effective impurity model corresponding to the action [20]

$$S_{\text{imp}} = \int d\tau d\tau' \Big\{ -\sum_\sigma f^\dagger_\sigma(\tau)\mathcal{G}^{-1}(\tau - \tau')f_\sigma(\tau') - \frac{1}{2}\boldsymbol{S}_f(\tau)\cdot\mathcal{J}(\tau - \tau')\boldsymbol{S}_f(\tau')\Big\} + \int d\tau U n_{f\uparrow}(\tau)n_{f\downarrow}(\tau), \tag{3}$$

where the repulsion U is taken to be infinite to exclude double occupation. The local electron is denoted by the Grassmann number f_σ, and we introduced $n_{f\sigma} = f^\dagger_\sigma f_\sigma$ and $\boldsymbol{S}_f = (1/2)\sum_{\sigma\sigma'} f^\dagger_\sigma \boldsymbol{\sigma}_{\sigma\sigma'} f_{\sigma'}$. The local propagator $\mathcal{G}$ and the local time-dependent exchange interaction $\mathcal{J}$ are determined by the self-consistency conditions [20]

$$\mathcal{G}^{-1}(i\omega_n) = i\omega_n + \mu - t^2 G_{\text{imp}}(i\omega_n), \tag{4}$$

$$\mathcal{J}(i\nu_n) = J^2\chi_{\text{imp}}(i\nu_n), \tag{5}$$

where G_{imp} is the single-particle Green function, and χ_{imp} is the spin susceptibility, both evaluated in the effective impurity model. Furthermore, ω_n and ν_n are fermionic and bosonic Matsubara frequencies, respectively. The self-consistency condition Eq. (5) corresponds to that of the extended DMFT [21,22,25,26] with semicircular density of couplings [27,28].

The first and second term in S_{imp} can be represented by fermionic and vector bosonic baths, respectively, which we express by the operators $a_{k\sigma}$ and $\boldsymbol{b}_q$. The corresponding Hamiltonian is written as

$$H_{\text{imp}} = -\mu n_f + U n_{f\uparrow}n_{f\downarrow} + \sum_{k\sigma}\epsilon_k a^\dagger_{k\sigma}a_{k\sigma} + \sum_q \omega_q \boldsymbol{b}^\dagger_q\cdot\boldsymbol{b}_q + V\sum_\sigma (f^\dagger_\sigma a_\sigma + a^\dagger_\sigma f_\sigma) + g\boldsymbol{S}_f\cdot(\boldsymbol{b} + \boldsymbol{b}^\dagger), \tag{6}$$

where $a_\sigma = N^{-1/2}\sum_k a_{k\sigma}$ and $\boldsymbol{b} = N^{-1/2}\sum_q \boldsymbol{b}_q$, with N as the number of sites. The quantities entering in H_{imp} are connected with those in S_{imp} by the relations

$$\Delta(i\omega_n) = \frac{V^2}{N}\sum_k \frac{1}{i\omega_n - \epsilon_k}, \tag{7}$$

$$\mathcal{J}(i\nu_n) = \frac{g^2}{N}\sum_q \frac{2\omega_q}{\nu_n^2 + \omega_q^2}, \tag{8}$$

with $\mathcal{G}^{-1}(i\omega_n) = i\omega_n + \mu - \Delta(i\omega_n)$.

Spin-boson coupling in CT-QMC.—We solve the effective impurity model Eq. (6) using the hybridization-expansion solver of the CT-QMC method [29]. An algorithm for the inclusion of a bosonic bath into the CT-QMC method was formulated by Werner and Millis in the case of impurity models with electron-phonon coupling [30,31]. They used the so-called Lang-Firsov transformation to eliminate the coupling term and thereby arrived at an efficient treatment of phonons. An *exchange* coupling cannot be eliminated in this way, since the spin operator $\boldsymbol{S}_f$ has three components which do not commute. For that reason, we treat the spin-boson coupling by a stochastic method. Namely, we perform a double expansion in terms of the hybridization and the spin-boson coupling, and evaluate the series by Monte Carlo sampling [32].

Results.—We now present the result of the model Eq. (1) as a function of the dimensionless coupling strength J/t, the particle density n, and the temperature T. In the following, energies are measured in units of $W = 2t = 1$, where W is the half-width of the density of states of the noninteracting model.

The quasiparticle renormalization factor $z = [1 - \text{Im}\Sigma(i\omega_0)/\omega_0]^{-1}$ is shown in Fig. 1(a) as a function of density n. While for $J = 0$, z tends to zero at $n = 1$, for $J/t = 0.5$, it approaches zero at $n \simeq 0.66 \equiv n_0$ with increasing slope. This behavior is contrast to the result in $M = \infty$, where z vanishes at $n = 1$ regardless of the value of J [20]. In the realistic case $M = 2$, the system hence appears to be a non-Fermi liquid for $n \gtrsim n_0$.

To identify the type of electronic state which is stable for $n \gtrsim n_0$, we calculate the residual moment defined by $\chi(\tau = \beta/2)$, which is equal to $T\chi$ in the limit $T \to 0$, but which approaches the $T = 0$ value faster than $T\chi$. The residual moment per electron is plotted in Fig. 1(b). The value at $n = 1$ corresponds to $S^2/3$, which is consistent with previous QMC calculations [14]. We see that $\chi(\beta/2)$ increases with decreasing T for $n \gtrsim n_0$, while it

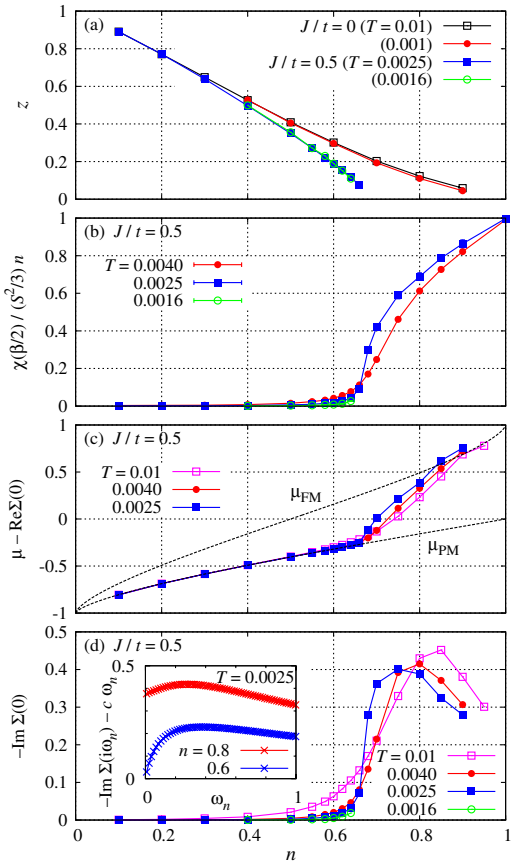

FIG. 1 (color online). Four physical quantities characterizing the paramagnetic state are plotted as a function of n: (a) the renormalization factor z, (b) the residual moment $\chi(\beta/2)$ per electron normalized by $S^2/3 = 12$, (c) the effective chemical potential $\mu_{\rm eff} \equiv \mu - {\rm Re}\Sigma(0)$, and (d) the scattering rate $-{\rm Im}\Sigma(0^+)$. The dashed curves in (c) show the chemical potential of the paramagnetic and polarized state, $\mu_{\rm PM}$ and $\mu_{\rm FM}$, for a noninteracting system. The inset in (d) shows $-{\rm Im}\Sigma(i\omega_n) - c\omega_n$ with $c = n/(2-n)$ [37].

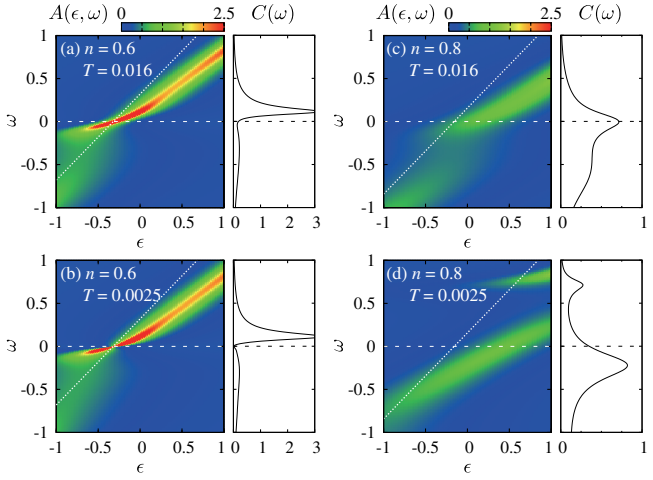

FIG. 2 (color online). Intensity plots of the single-particle excitation spectrum $A(\epsilon, \omega)$, and the "atomic spectrum" $C(\omega)$ for $J/t = 0.5$, $n = 0.6$, 0.8, and $T = 0.0025$, 0.016. The dotted line shows the energy dispersion of the noninteracting system.

decreases for $n \lesssim n_0$. From this data, we conclude that the phase has a residual moment for $n \gtrsim n_0$.

Next, we compute the momentum-resolved single-particle excitation spectrum $A(\epsilon, \omega)$, which is defined in terms of the local self-energy $\Sigma(i\omega_n) = \mathcal{G}^{-1}(i\omega_n) - G^{-1}_{\rm imp}(i\omega_n)$ by

$$A(\epsilon, \omega) = -\frac{1}{\pi}\,{\rm Im}\frac{1}{\omega^+ + \mu - \epsilon - \Sigma(\omega^+)}. \qquad (9)$$

Here, $\epsilon \equiv \epsilon_k$, with $\epsilon[-W, W]$, is the dispersion in $d = \infty$ which can be used to parameterize the momentum dependence. We performed the analytical continuation to $\omega^+ = \omega + i0$ by a Padé approximation [33]. The results are shown in Fig. 2. For $n = 0.6$, i.e., in the Fermi liquid regime [Figs. 2(a) and 2(b)], quasiparticle excitations are seen to occur around the Fermi energy. Figures 2(c) and 2(d) show the spectra for $n = 0.8$, i.e., for the state with a residual moment. At the higher temperature, the dispersion is similar to that in the Fermi-liquid regime, but the spectral features are less sharp than those for $n = 0.6$. In fact, they do not become sharper even for the lowest temperature of our calculation [Fig. 2(d)]. We conclude from these results, that the phase close to half filling corresponds to an *incoherent* metallic state with a residual moment.

The spectrum shown in Fig. 2(d) has very remarkable features. Firstly, the broad spectrum crosses the Fermi level at the "momentum" ϵ which is larger than its value for the noninteracting case. Secondly, there is an additional band above the broad spectrum. We now discuss these features in more detail. The effective chemical potential $\mu_{\rm eff} = \mu - {\rm Re}\Sigma(0)$, which is related to the Fermi-surface volume if ${\rm Im}\Sigma(0) = 0$, is shown in Fig. 1(c) together with the chemical potentials of the paramagnetic and polarized state, $\mu_{\rm PM}$ and $\mu_{\rm FM}$, in the noninteracting system ($U = J = 0$). For $n \lesssim n_0$, $\mu_{\rm eff}$ agrees with $\mu_{\rm PM}$, indicating that the Luttinger theorem is satisfied. On the other hand, it starts to deviate from $\mu_{\rm PM}$ at $n \simeq n_0$ and approaches $\mu_{\rm FM}$. We note that this deviation does not imply a violation of the Luttinger theorem, since there is no discontinuity in the momentum distribution function in this regime. Namely, for densities $n \gtrsim n_0$, the scattering rate $-{\rm Im}\Sigma(0^+)$ does not tend to zero for temperatures down to $T = 0.0025$ [Fig. 1(d)]. This is also explicitly seen in the ω_n dependence of ${\rm Im}\Sigma(i\omega_n)$ [inset of Fig. 1(d)].

The origin of the additional band observed in Fig. 2(d) can be explained as follows. The weights of the upper and lower Hubbard band vary according to $n/2$. Hence, upon hole doping some weight is transferred from the Hubbard bands to energies just above the lower band edge, leading to an additional spectral weight $\delta = 1 - n$ [34]. This additional spectrum is due to the hole dynamics. In Fig. 2(d), the hole spectrum is separated from the lower Hubbard

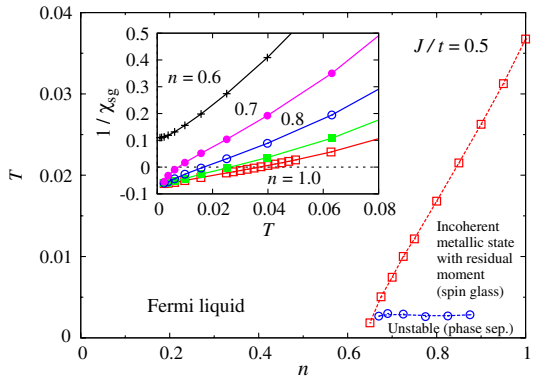

FIG. 3 (color online). Temperature vs density phase diagram of the random coupling t-J model in $d = \infty$ for $J/t = 0.5$. The blue dashed curve denotes the boundary of a phase separated region. The red dashed curve indicates the transition to a spin-glass state. The inset shows the inverse of the spin-glass susceptibility $\chi_{\rm sg}$ as a function of T.

band, while in the coherent Fermi liquid regime, the two mix. Hence, the appearance of the additional band in Fig. 2(d) indicates the incoherence of the holes. This is also clearly expressed by the "atomic spectrum" $C(\omega) = -(1/\pi)\mathrm{Im}[\omega^+ + \mu - \Sigma(\omega^+)]^{-1}$ in Fig. 2. For $n = 0.6$, $C(\omega)$ shows a single sharp peak corresponding to the coherent band, while for $n = 0.8$, it consists of two slightly broader peaks corresponding to the two-band structure. A similar single-particle spectrum was observed for a single hole in the two-dimensional t-J model [35].

At this point, a comment on the possible ground state near half filling is in order. The incoherent metallic state has a residual entropy, and therefore, an instability is expected to take place to lift the degeneracy. Indeed, in our calculation with a paramagnetic bath, we found a divergence of the charge compressibility $\partial n/\partial\mu$ below $T \lesssim 0.003$, indicating that the paramagnetic solution is unstable against phase separation. The temperature at which $\partial\mu/\partial n$ changes sign is plotted in Fig. 3 (blue dashed curve). Phase separation has also been found in the one-dimensional t-J model for large-J [36]. Another possibility is magnetic symmetry breaking. Furthermore, it is known that at half filling a spin-glass transition, i.e., the breaking of the replica symmetry, occurs [10–12,14–16], while long-range magnetic order is suppressed due to the random distribution of the exchange interaction. To estimate the spin-glass transition temperature $T_{\rm sg}$, we evaluate the spin-glass susceptibility $\chi_{\rm sg}$ using the expression

$$\chi_{\rm sg} = \chi_{\rm imp}^2/(1 - J^2\chi_{\rm imp}^2), \tag{10}$$

derived at half filling [16]. In the inset of Fig. 3, the temperature dependence of $1/\chi_{\rm sg}$ is shown. The transition temperature $T_{\rm sg}$ itself is plotted in Fig. 3 (red dashed curve). At $n = 1$, we obtain $T_{\rm sg}/J \approx 0.147$, which is consistent with the result of Ref. [14]. Upon doping, $T_{\rm sg}$ decreases monotonically and reduces to zero at $n \simeq 0.635$, a value which is close to n_0. Therefore, the incoherent metallic state is actually located in the region where the spin-glass phase can be expected to be stable. That is, the incoherent metallic state may be stabilized if the spin-glass transition is suppressed. Nevertheless, the peculiar spectrum in this regime is still physically meaningful, since the divergence of $\chi_{\rm sg}$ does not affect the self-consistency equations. This is the same as in the case of the paramagnetic DMFT solution of the Hubbard model, which is found in the region where actually the antiferromagnetic phase is stable [9].

In summary, we presented the exact numerical solution of the t-J model with random exchange couplings in $d = \infty$. Near half filling, the solution corresponds to an incoherent metal with a residual moment. The single-particle excitations not only lead to a broad spectrum crossing the Fermi level, but to an additional band at higher energies. Because of the residual moment, the effective chemical potential is located close to the Fermi level of the polarized noninteracting system. The additional band is observed only in the non-Fermi liquid regime, and is a signature of the incoherence of the holes.

Finally, we comment on the t-J model with *nonrandom* couplings in $d = 2$, 3. Equations (4) and (5) may be regarded as a single-site approximation for models in $Z < \infty$ [28]. Indeed, we obtained preliminary results for the same quantities as shown in Fig. 1 in $d = 2$ and 3 which indicate that the paramagnetic solution near half filling is again an incoherent metal with a residual moment. The case $d < \infty$, including symmetry broken solutions, e.g., the antiferromagnetic or the spin-glass state, will be investigated in the future.

We thank A. Georges, Y. Kuramoto, T. Pruschke, and G. Zaránd for useful discussions. Support of J. O. by a JSPS Postdoctoral Fellowship for Research Abroad, and by the Deutsche Forschungsgemeinschaft through TRR 80 is gratefully acknowledged.

[1] M. Imada, A. Fujimori, and Y. Tokura, Rev. Mod. Phys. **70**, 1039 (1998).
[2] P. Lee, N. Nagaosa, and X.-G. Wen, Rev. Mod. Phys. **78**, 17 (2006).
[3] J. Kokalj and P. Prelovsek, Phys. Rev. B **75**, 045111 (2007).
[4] W. O. Putikka, M. U. Luchini, and R. R. P. Singh, Phys. Rev. Lett. **81**, 2966 (1998).
[5] P. Phillips, Ann. Phys. (Amsterdam) **321**, 1634 (2006).
[6] S. Sakai, Y. Motome, and M. Imada, Phys. Rev. Lett. **102**, 056404 (2009).
[7] B. S. Shastry, Phys. Rev. B **81**, 045121 (2010).
[8] W. Metzner and D. Vollhardt, Phys. Rev. Lett. **62**, 324 (1989).
[9] A. Georges, G. Kotliar, W. Krauth, and M. J. Rozenberg, Rev. Mod. Phys. **68**, 13 (1996).

[10] D. Sherrington and S. Kirkpatrick, Phys. Rev. Lett. **35**, 1792 (1975).
[11] D. J. Thouless, P. W. Anderson, and R. G. Palmer, Philos. Mag. **35**, 593 (1977).
[12] A. J. Bray and M. A. Moore, J. Phys. C **13**, L655 (1980).
[13] S. Sachdev and J. Ye, Phys. Rev. Lett. **70**, 3339 (1993).
[14] D. R. Grempel and M. J. Rozenberg, Phys. Rev. Lett. **80**, 389 (1998).
[15] A. Georges, O. Parcollet, and S. Sachdev, Phys. Rev. Lett. **85**, 840 (2000).
[16] A. Georges, O. Parcollet, and S. Sachdev, Phys. Rev. B **63**, 134406 (2001).
[17] C. M. Varma, P. B. Littlewood, S. Schmitt-Rink, E. Abrahams, and A. E. Ruckenstein, Phys. Rev. Lett. **63**, 1996 (1989).
[18] F. C. Chou, N. R. Belk, M. A. Kastner, R. J. Birgeneau, and A. Aharony, Phys. Rev. Lett. **75**, 2204 (1995).
[19] Subsequent studies of the SU(M) random coupling Heisenberg model within DMFT for $M = 2$ by quantum Monte Carlo [14] and by a $1/M$ expansion [15,16] did not find marginal Fermi-liquid behavior.
[20] O. Parcollet and A. Georges, Phys. Rev. B **59**, 5341 (1999).
[21] J. L. Smith and Q. Si, Phys. Rev. B **61**, 5184 (2000).
[22] K. Haule, A. Rosch, J. Kroha, and P. Wölfle, Phys. Rev. B **68**, 155119 (2003).
[23] The Hamiltonian (1) in $Z = \infty$ is equivalent to a t-J model on a fully connected lattice with random hopping and random exchange interactions. This correspondence was demonstrated for the Ising model in Ref. [24].
[24] A. Georges, M. Mézard, and J. S. Yedidia, Phys. Rev. Lett. **64**, 2937 (1990).
[25] Y. Kuramoto and N. Fukushima, J. Phys. Soc. Jpn. **67**, 583 (1998).
[26] P. Sun and G. Kotliar, Phys. Rev. B **66**, 085120 (2002).
[27] This correspondence follows from the fact that the eigenvalues of the random matrix J_{ij} with matrix elements J_{ij} distributed according to (2), have a semi-circular distribution with half-width $2J$ [11].
[28] We note that when Eq. (5) is applied to models without randomness, the coupling constants should be scaled as $J_{ij} \sim 1/Z$ to keep the magnetic transition temperature finite. In this case, the equation incorporates all the terms of order $1/Z$ as well as higher-order terms within a single-site approximation [25].
[29] For a review, see E. Gull, A. J. Millis, A. I. Lichtenstein, A. N. Rubtsov, M. Troyer, and P. Werner, Rev. Mod. Phys. **83**, 349 (2011).
[30] P. Werner and A. J. Millis, Phys. Rev. Lett. **99**, 146404 (2007).
[31] P. Werner and A. J. Millis, Phys. Rev. Lett. **104**, 146401 (2010).
[32] J. Otsuki, Phys. Rev. B **87**, 125102 (2013).
[33] Here a Padé approximation is possible because the CT-QMC data have very little statistical noise.
[34] M. B. J. Meinders, H. Eskes, and G. A. Sawatzky, Phys. Rev. B **48**, 3916 (1993).
[35] For a review, see E. Dagotto, Rev. Mod. Phys. **66**, 763 (1994).
[36] M. Ogata, M. U. Luchini, S. Sorella, and F. F. Assaad, Phys. Rev. Lett. **66**, 2388 (1991).
[37] At $U = \infty$ the self-energy $\Sigma(i\omega_n)$ has the high-frequency behavior $\Sigma(i\omega_n) \sim (1 - 1/a)i\omega_n$, which originates in $G(i\omega_n) \sim a/i\omega_n$ with $a = 1 - n/2$. We subtracted this term in the plot.